Table S1: Modeling scenarios

Name	Emissions scenario	PFAL hydration?	Emissions FTOH%	Emissions FTI%	Emissions FTO%
BASE	Mean	Yes	48	4	48
HIGH_EMIS	High	Yes	48	4	48
LOW_EMIS	Low	Yes	48	4	48
FTO_ONLY	Mean	Yes	0	0	100
NO_HYDR	Mean	No	48	4	48
FTOH_ONLY	Mean	Yes	100	0	0
FTOH_NO_HYDR	Mean	No	100	0	0
FTO_NO_HYDR	Mean	No	0	0	100
NO_HYDR_LOW	Low	No	48	4	48
FTO_HIGH	High	Yes	0	0	100

Figure S1: Time series of modeled (bounds in grey) and observed (blue dots) annual deposition of C5-C11 PFCAs at Devon Ice Cap.

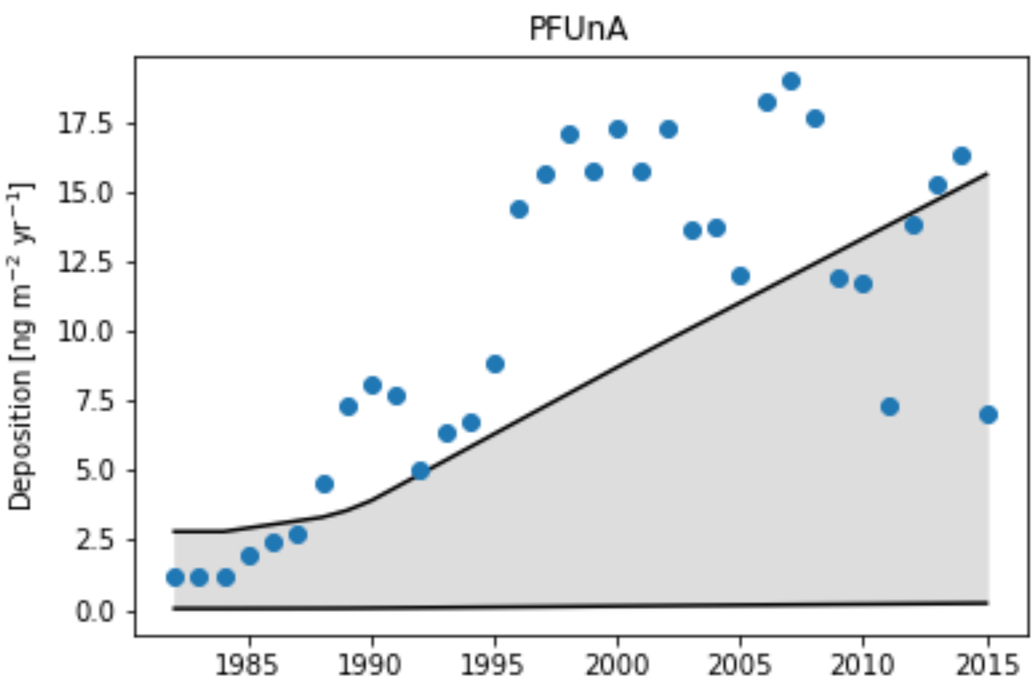

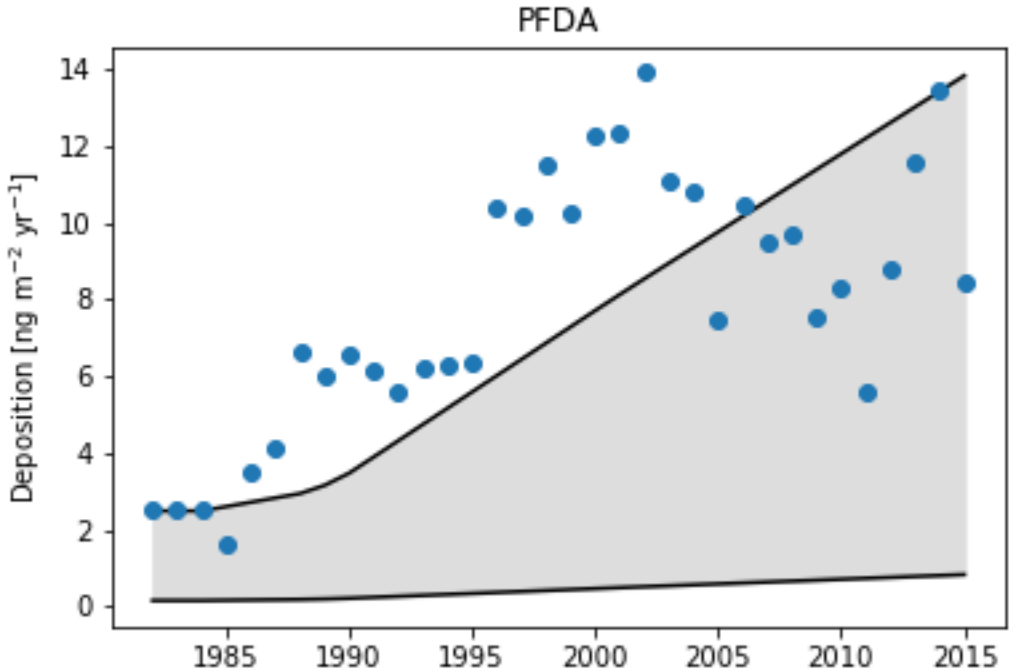

PFDA
Deposition [ng m^{-2} yr^{-1}]
0
2
4
6
8
10
12
14
1985
1990
1995
2000
2005
2010
2015

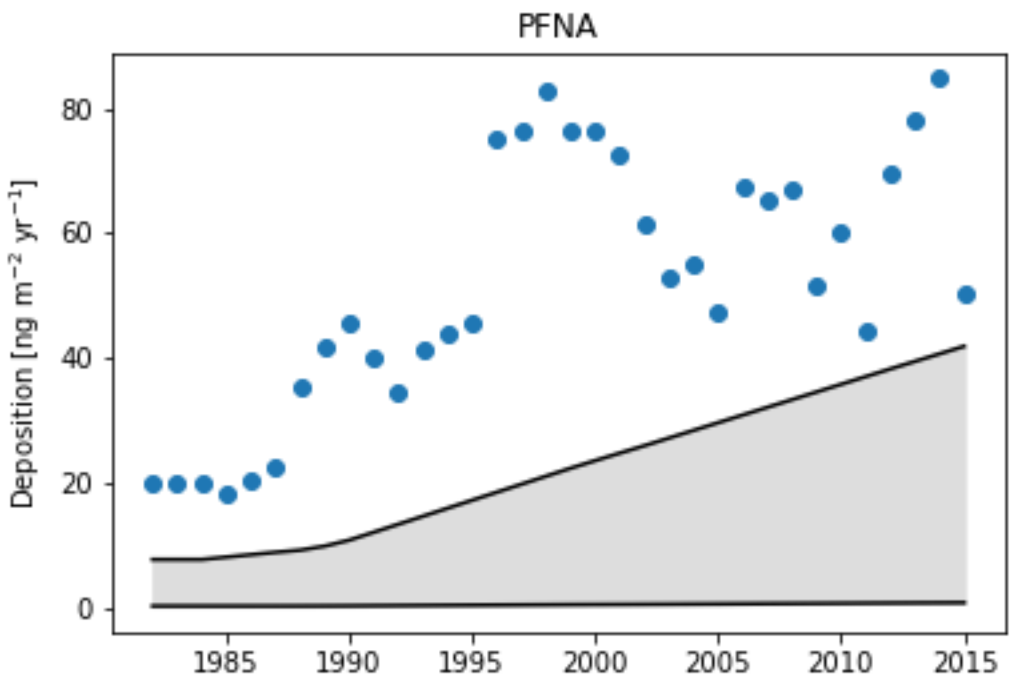

PFNA
Deposition [ng m^{-2} yr^{-1}]
0
20
40
60
80
1985
1990
1995
2000
2005
2010
2015

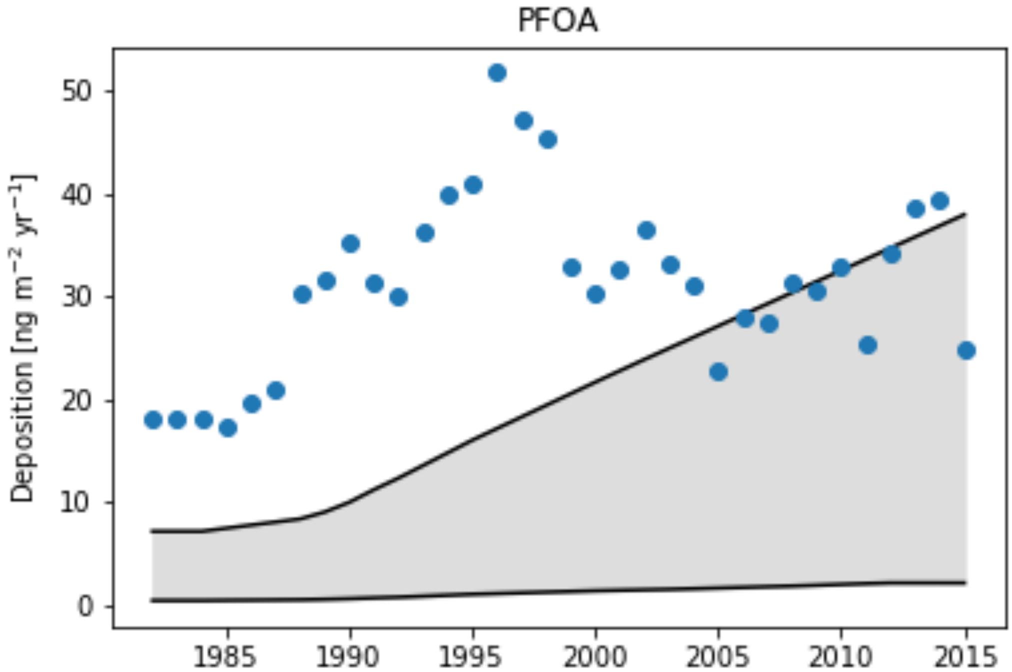
PFOA
Deposition [ng m⁻² yr⁻¹]
0
10
20
30
40
50
1985
1990
1995
2000
2005
2010
2015

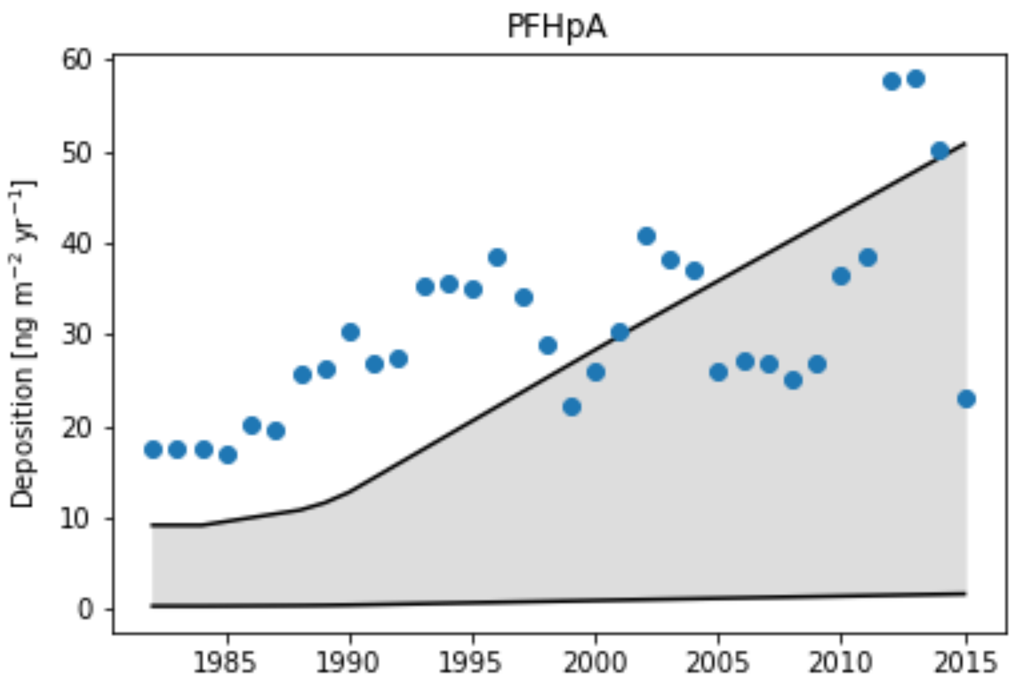
PFHpA
Deposition [ng m⁻² yr⁻¹]
0
10
20
30
40
50
60
1985
1990
1995
2000
2005
2010
2015

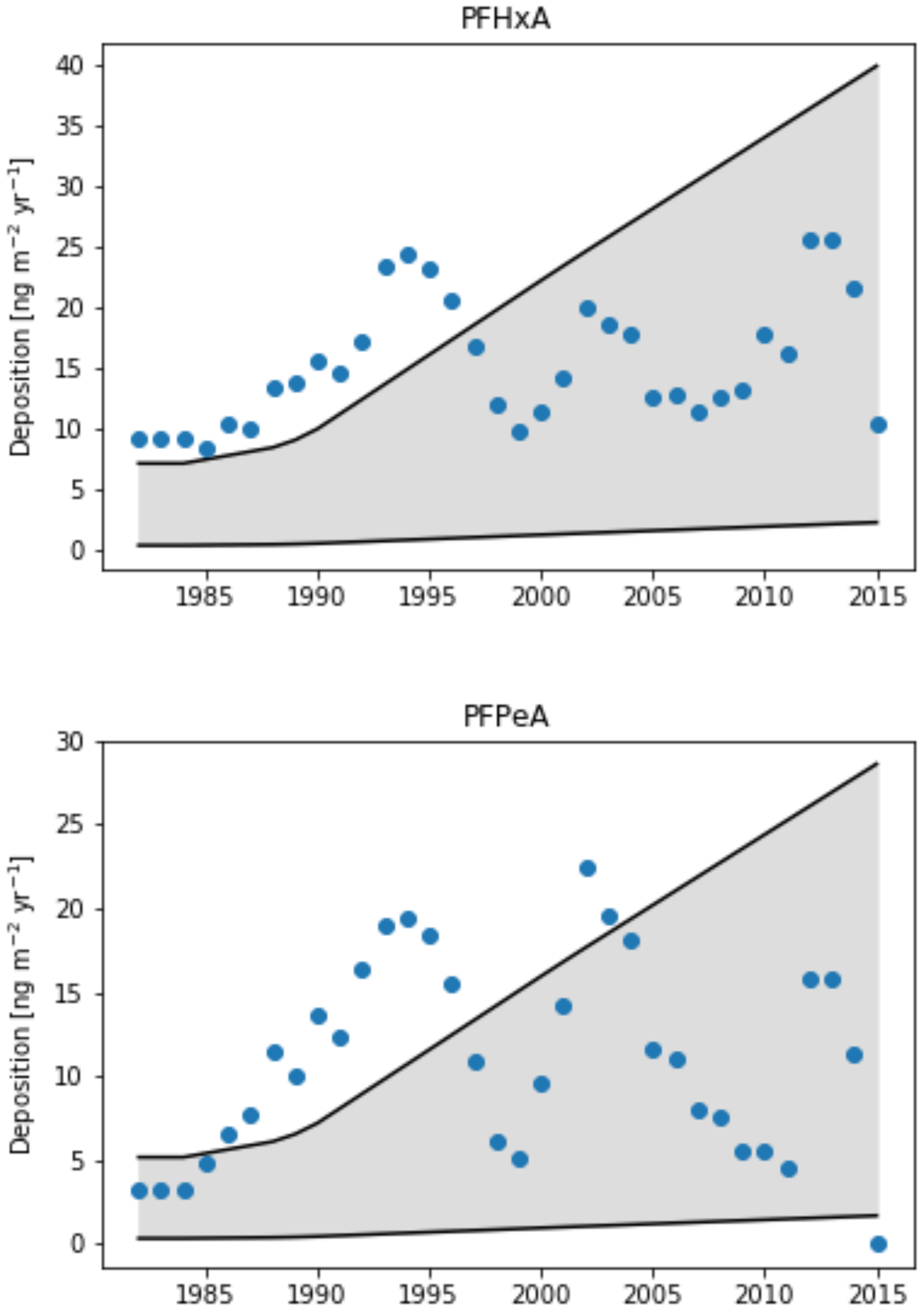
PFHxA
Deposition [ng m^{-2} yr^{-1}]
40
35
30
25
20
15
10
5
0
1985
1990
1995
2000
2005
2010
2015
PFPeA
Deposition [ng m^{-2} yr^{-1}]
30
25
20
15
10
5
0
1985
1990
1995
2000
2005
2010
2015

Table S2: Rainwater measurements

See RainwaterData.xlsx for data.

References:

Scott et al., Environ Sci Technol 2006, 40, 23, 7167-7174
Kwok et al., Environ Sci Technol 2010, 44, 7043-7049
Kirchgeorg et al., Environ Pollut 2013, 178, 367-374
Barton et al., J Environ Monitor 2007, 9, 839-846
Kim et al., Environ Sci Technol 2007, 41, 8328-8334
Loos et al., Anal Bioanal Chem 2007, 387, 1469-1478
Taniyasu et al., Anal Chim Acta 2008, 619, 221-230
Liu et al., Chin Sci Bull 2009, 54, 2440-2445
Liu et al., Environ International 2009, 35, 737-742
Mahmoud et al., Chemosphere 2009, 74, 467-472
Murakami et al., Chemosphere 2009, 74, 487-493
Dreyer et al., Environ Pollut 2010, 158, 1221-1227
Kwok et al., Environ Sci Technol 2010, 44, 7043-7049
Scott et al., J Great Lakes Res 2010, 36, 277-284
Zhang et al., Anal Chem 2010, 82, 2363-2373
Meyer et al., Environ Sci Technol 2011, 45, 8113-8119
Muller et al., Environ Sci Technol 2011, 45, 9901-9909
Nguyen et al., Chemosphere 2011, 82, 1277-1285
Nishikoori et al., Chemosphere 2011, 84, 1125-1132
Zhao et al., Microchem J 2011, 98, 207-214

Representativeness Error

Representativeness error is the relative error associated with comparison of a larger-scale average quantity with a single point measurement within that larger area. We calculate this error using:

$$\varepsilon_{IJ}^{h} = \frac{1}{N}\sum_{i=I-1}^{I+1}\sum_{j=J-1}^{J+1}\frac{abs(F_{ij}^{h} - F_{IJ}^{h})}{F_{IJ}^{h}}$$

where ε_{IJ}^{h} is the representativeness error for homolog h at model grid cell IJ, where I and J are the zonal and meridional indices of the grid cell, F_{IJ}^{h} is the deposition flux of homolog h at model grid cell IJ, and $N = 8$ is the number of adjacent grid cells. This calculation assumes that the variability between adjacent model grid boxes is representative of the variability within a model grid box, in the absence of other variability information.

Figure S2. 2015 annual average deposition of C3-C13 PFCA homologs.

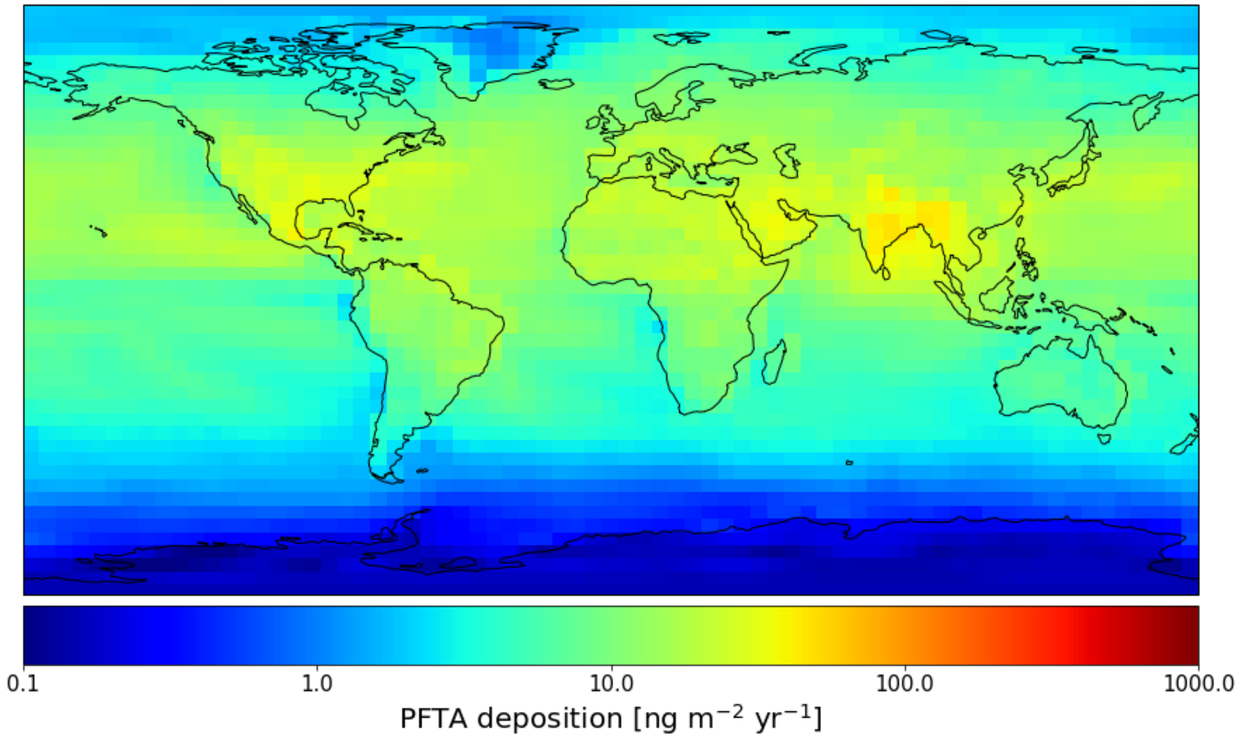

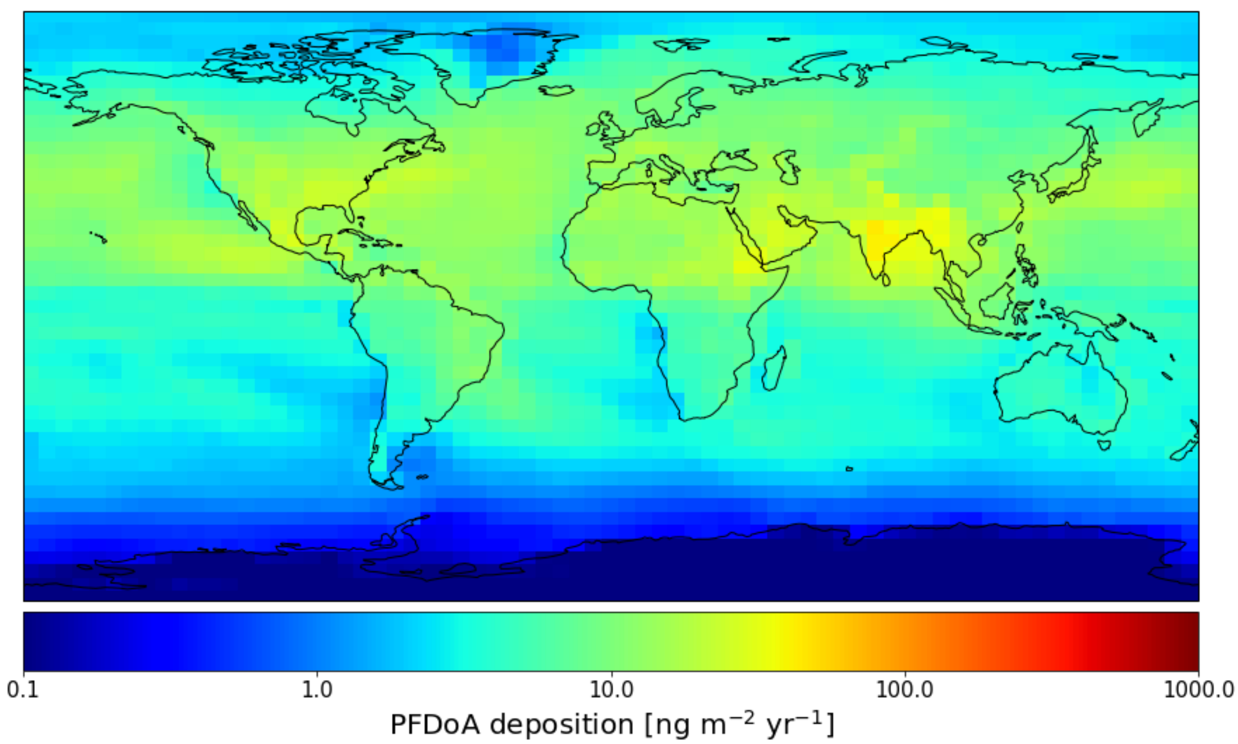

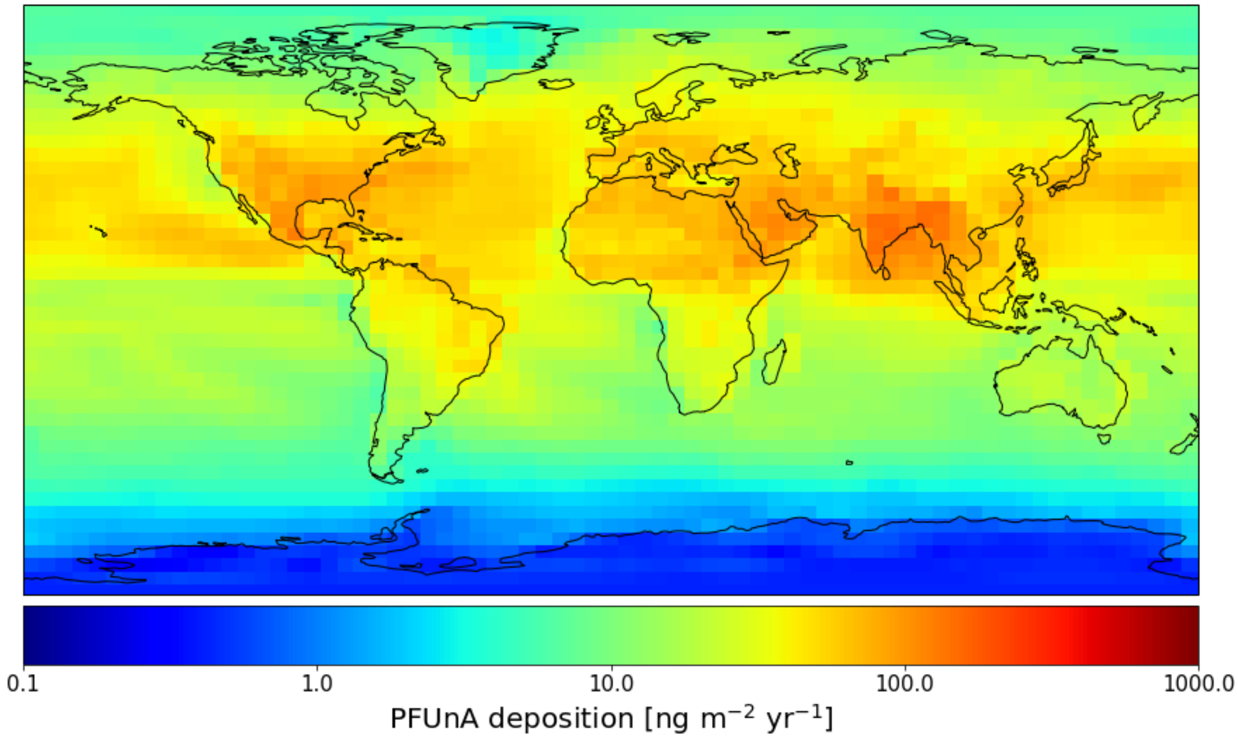
0.1
1.0
10.0
100.0
1000.0
PFUnA deposition [ng m^{-2} yr^{-1}]

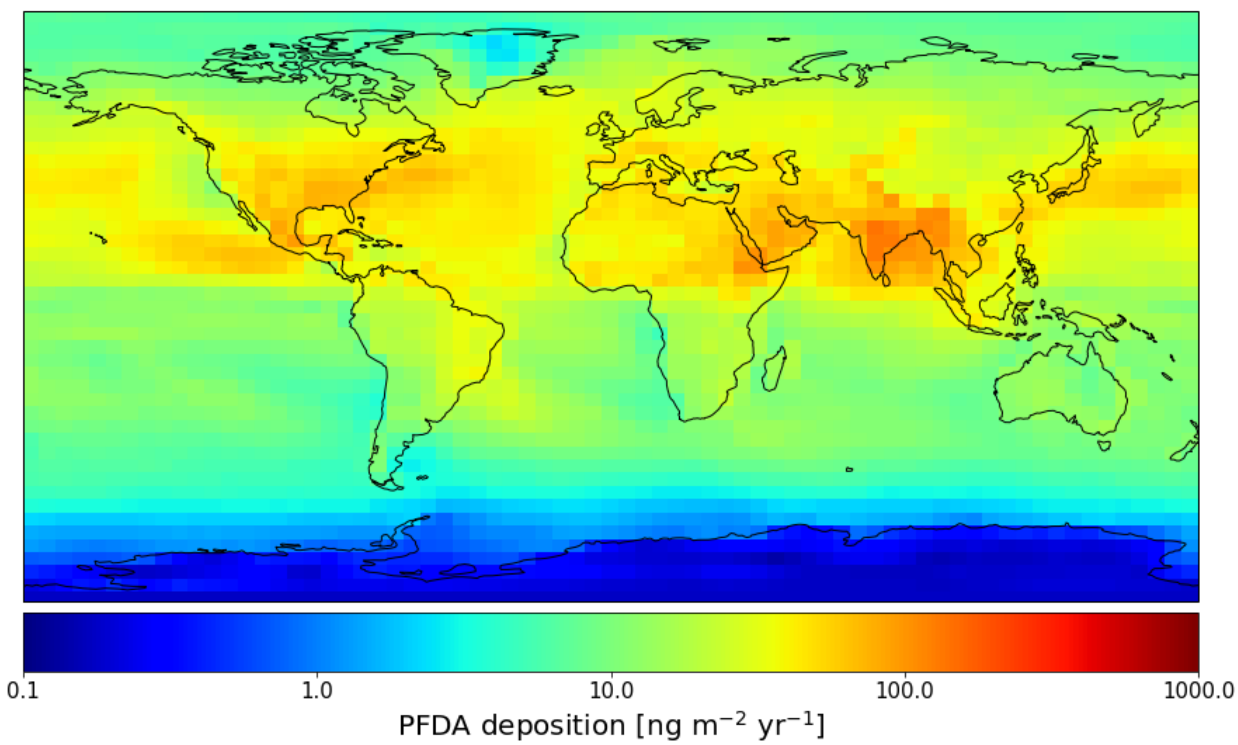
0.1
1.0
10.0
100.0
1000.0
PFDA deposition [ng m^{-2} yr^{-1}]

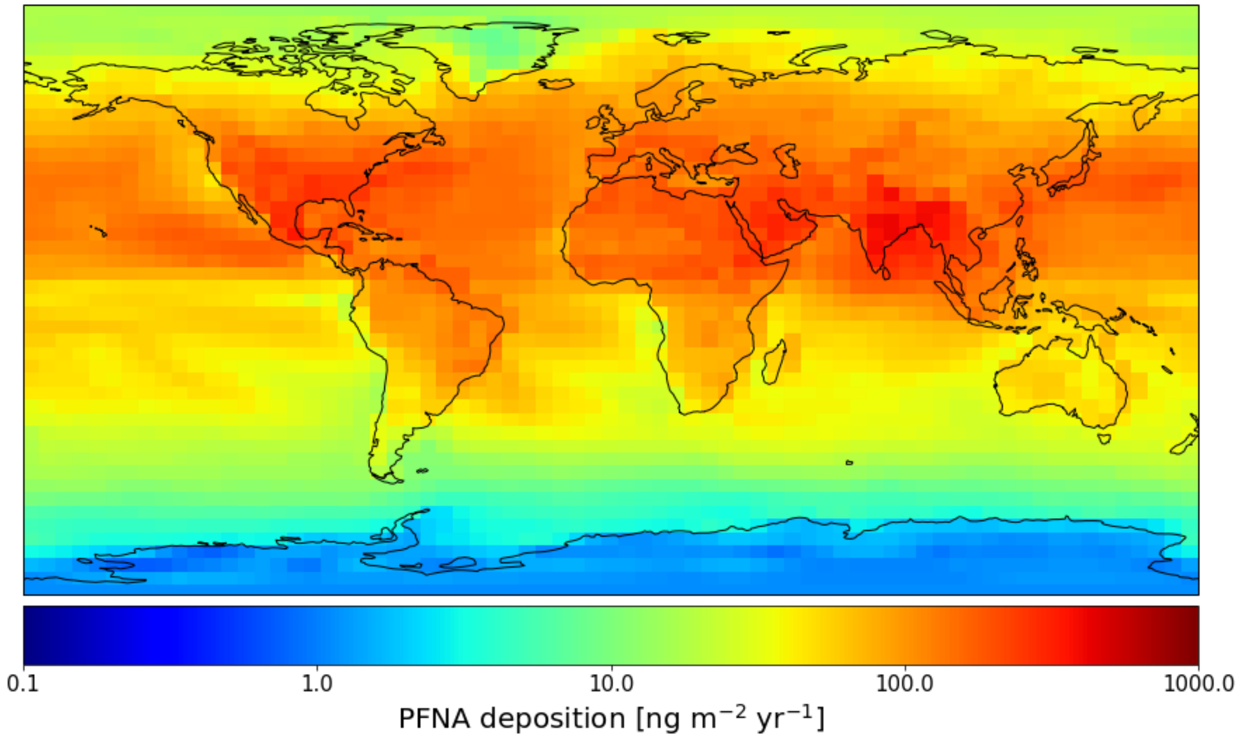
0.1
1.0
10.0
100.0
1000.0
PFNA deposition [ng m^{-2} yr^{-1}]

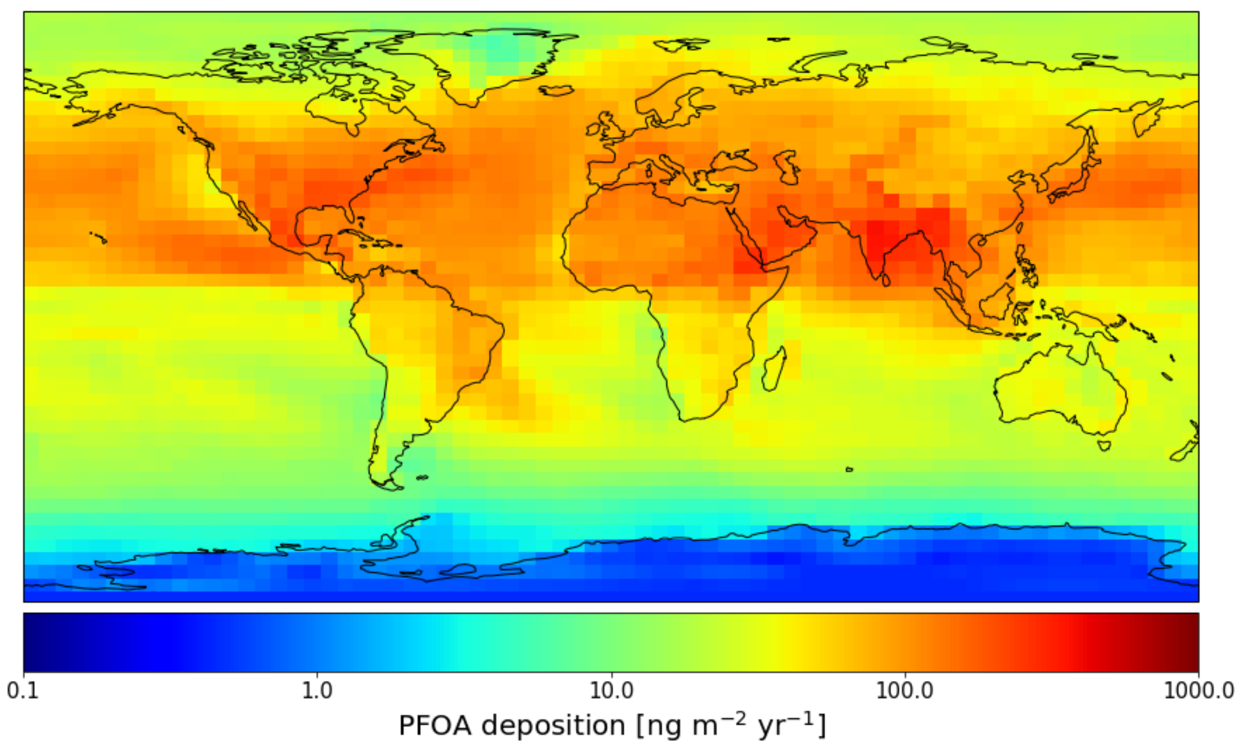
0.1
1.0
10.0
100.0
1000.0
PFOA deposition [ng m^{-2} yr^{-1}]

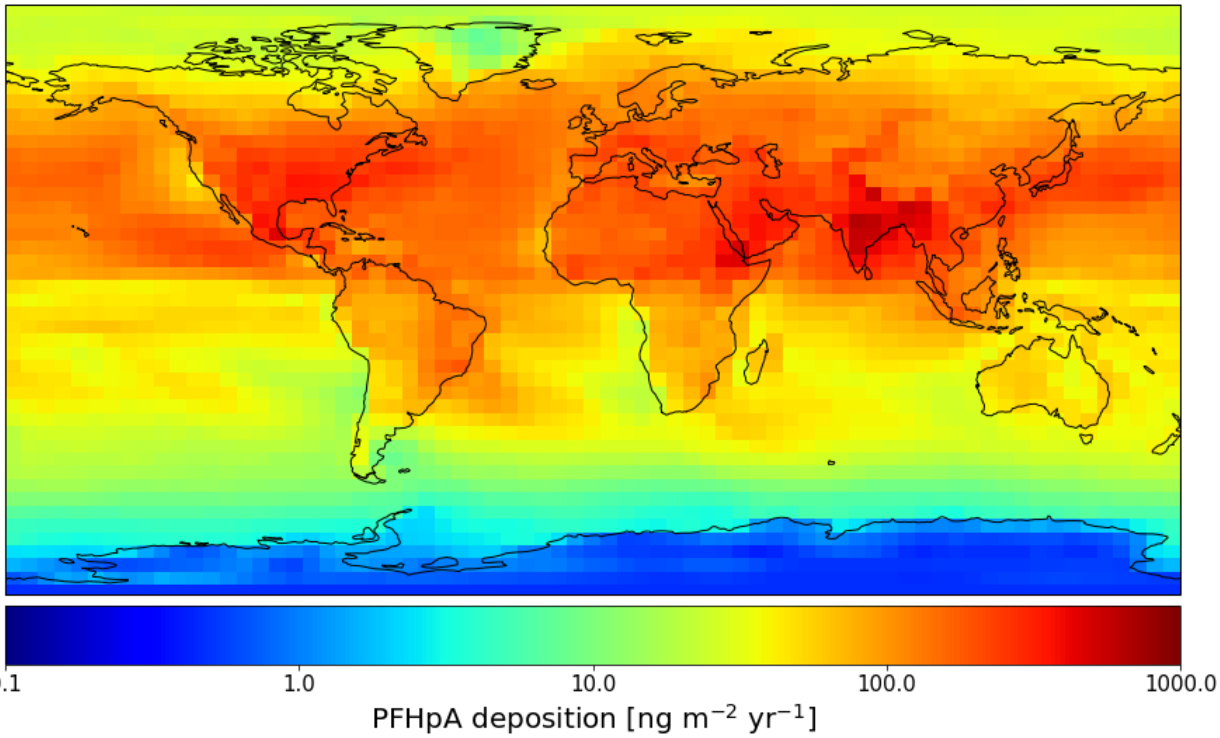
0.1
1.0
10.0
100.0
1000.0
PFHpA deposition [ng m^{-2} yr^{-1}]

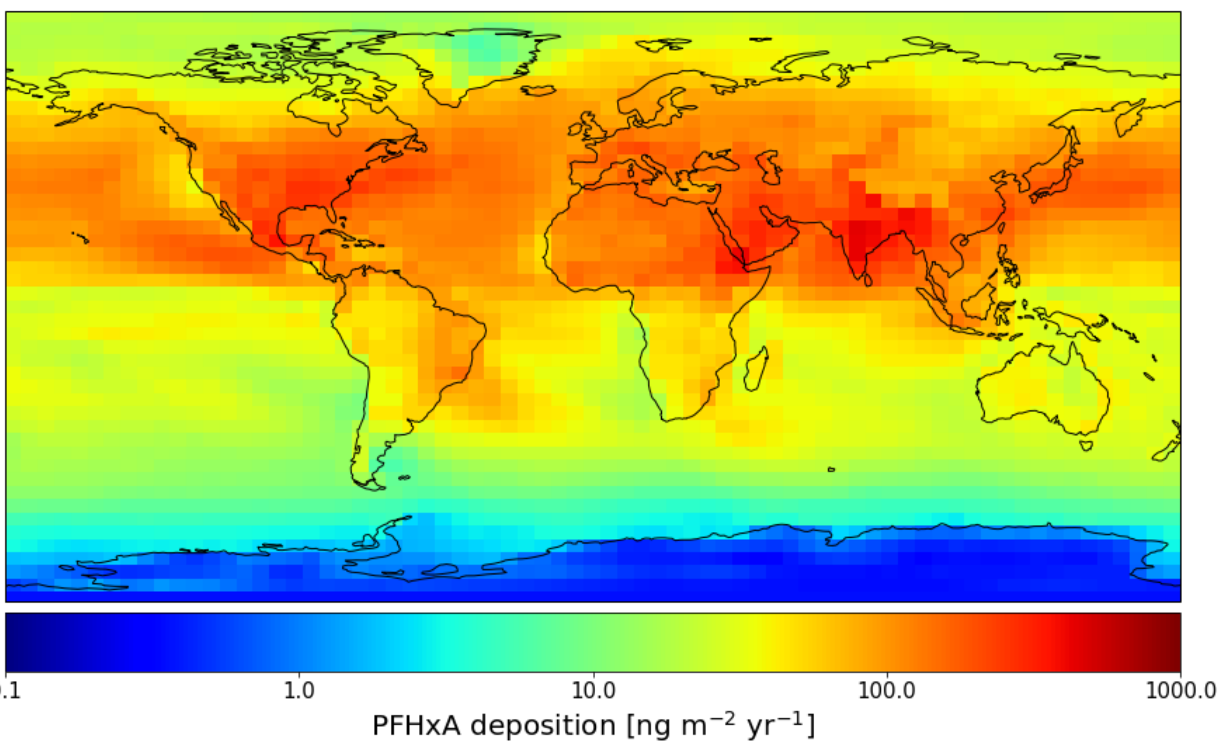
0.1
1.0
10.0
100.0
1000.0
PFHxA deposition [ng m^{-2} yr^{-1}]

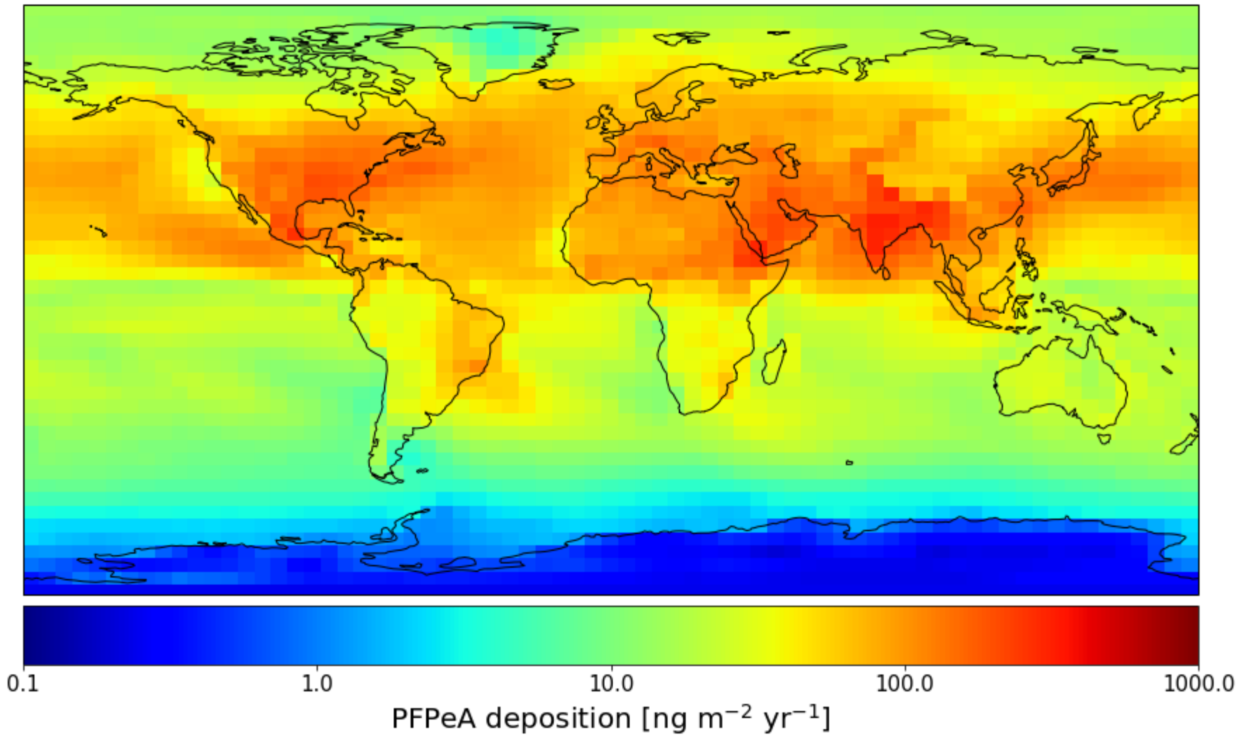
0.1
1.0
10.0
100.0
1000.0
PFPeA deposition [ng m^{-2} yr^{-1}]

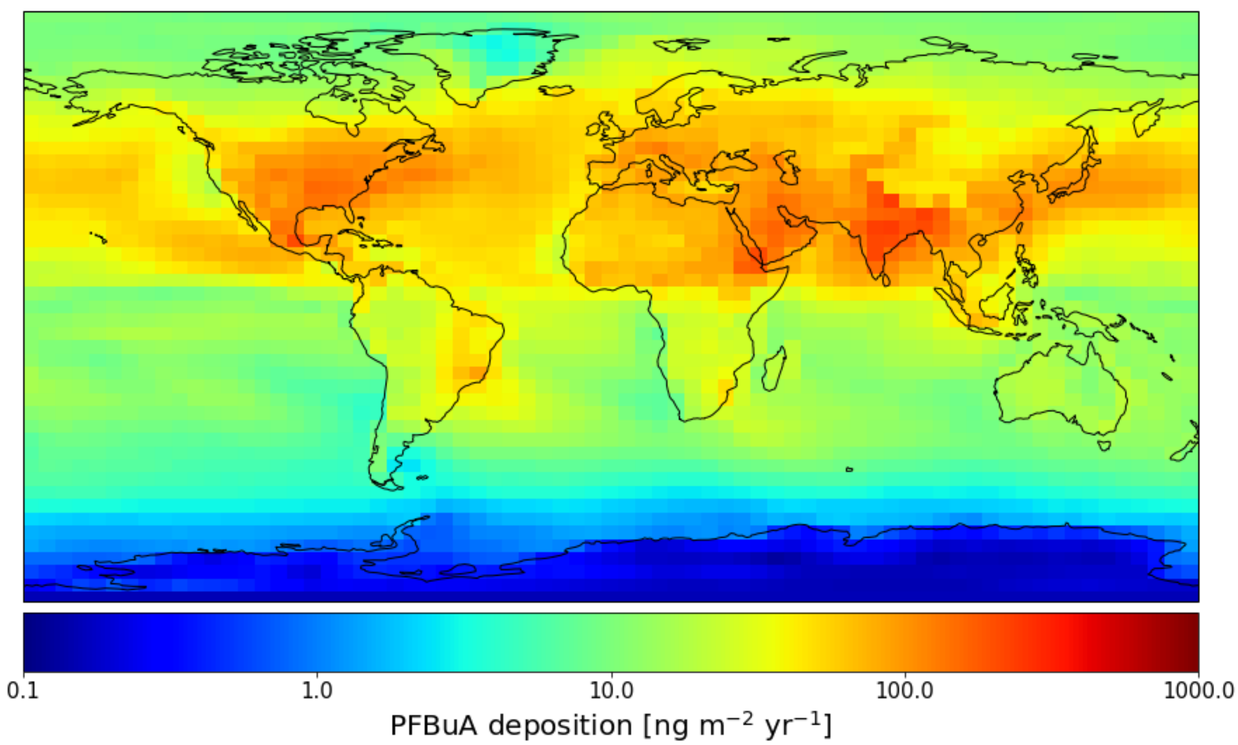
0.1
1.0
10.0
100.0
1000.0
PFBuA deposition [ng m^{-2} yr^{-1}]

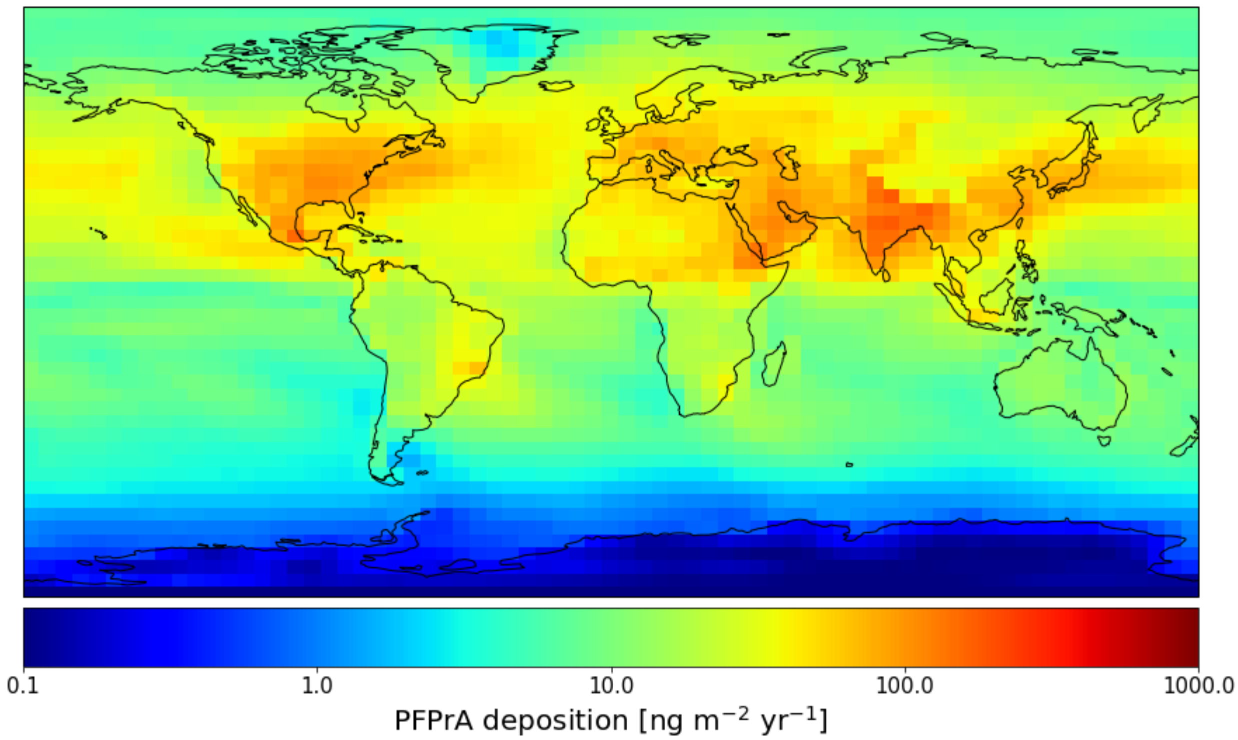
0.1
1.0
10.0
100.0
1000.0
PFPrA deposition [ng m−2 yr−1]

Figure S3. Percentage of total deposition contributed by wet deposition for PFOA, PFCAs longer than C8, and PFCAs shorter than C8.

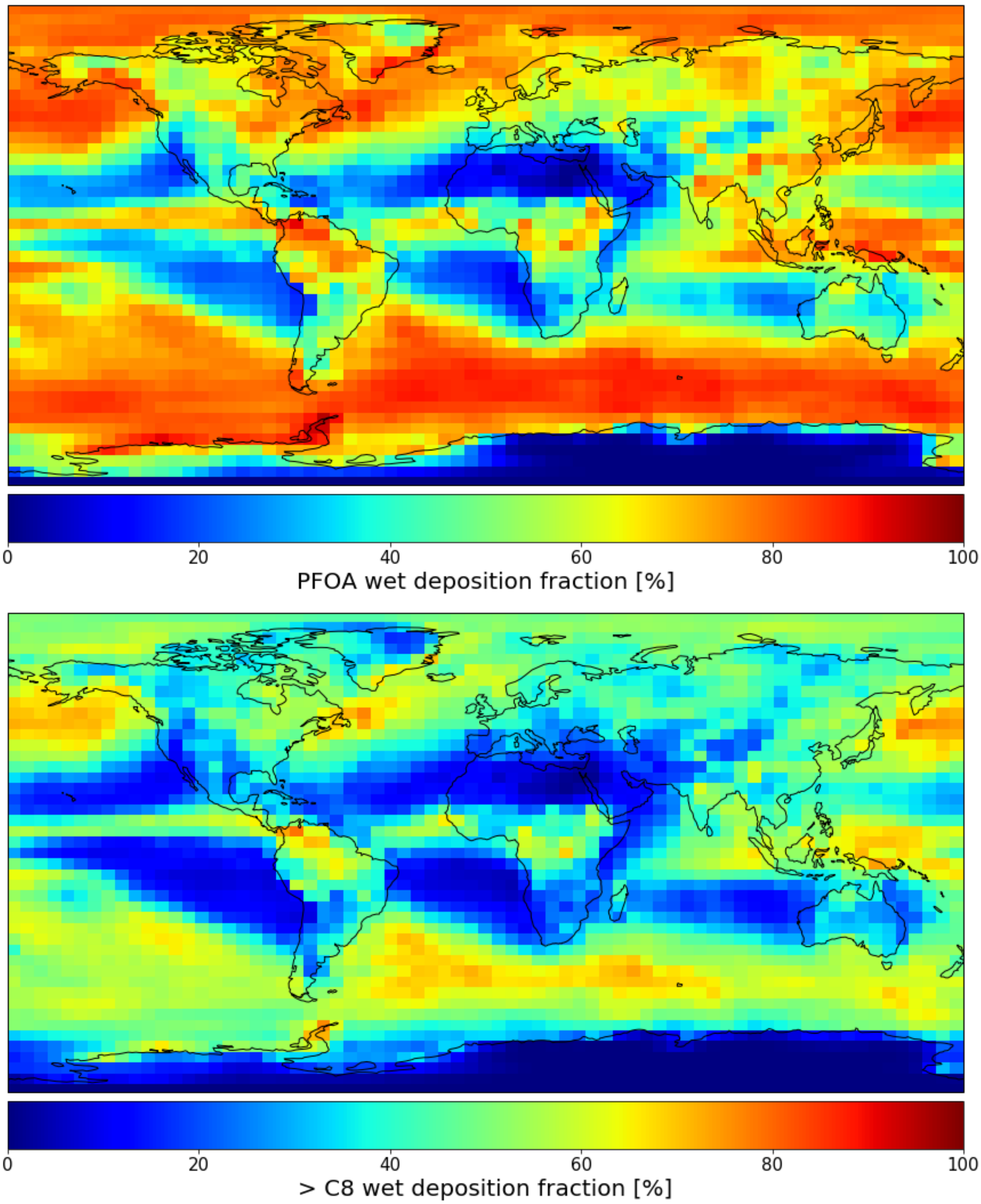

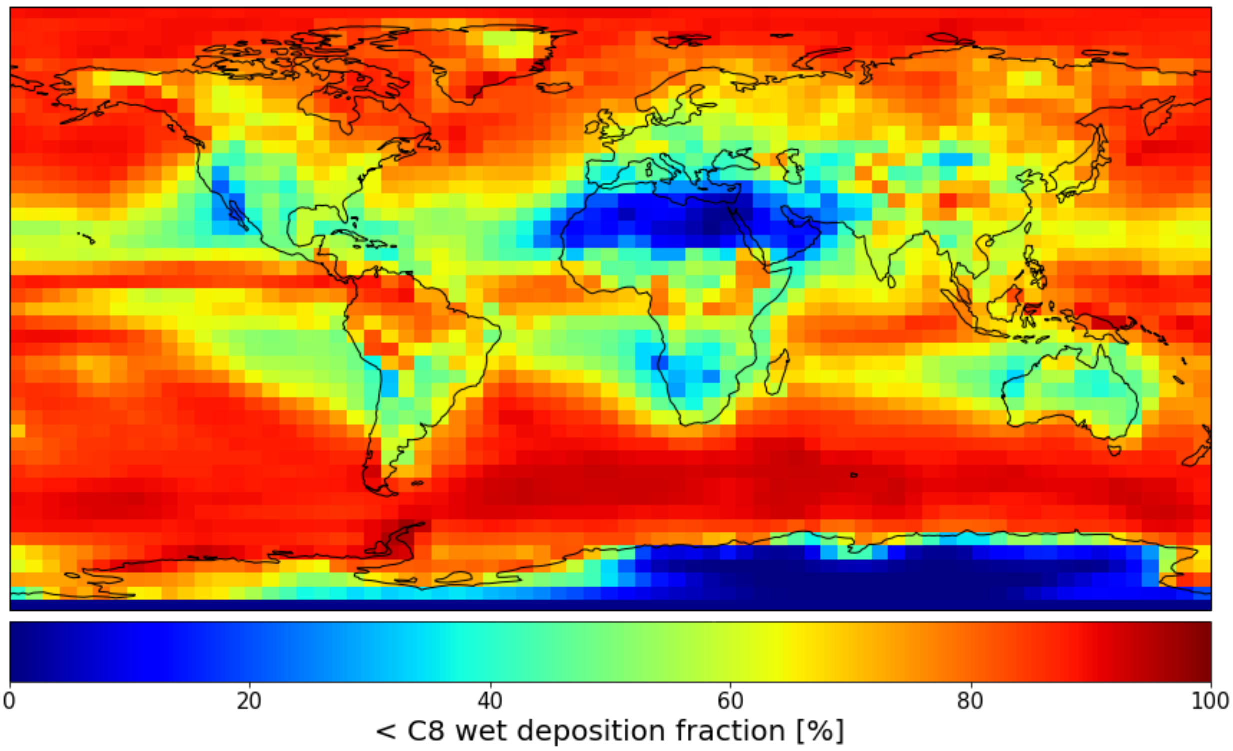
0
20
40
60
80
100
< C8 wet deposition fraction [%]

Table S3. List of reactions

1	$C_xF_{2x+1}CH_2C(O)H + h\nu \rightarrow C_xF_{2x+1}CH_2OO$	1.5×10^{-21} (cm^2 $photon^{-1}$ s^{-1})	a
2	$C_xF_{2x+1}CH_2C(O)H + OH \rightarrow C_xF_{2x+1}CH_2(O)OO$	2.0×10^{-12} (cm^3 s^{-1})	a
3	$C_xF_{2x+1}CH_2C(O)H + Cl \rightarrow C_xF_{2x+1}CH_2(O)OO$	1.9×10^{-11} (cm^3 s^{-1})	a
4	$C_xF_{2x+1}CH_2C(O)OO + NO_2 \rightarrow C_xF_{2x+1}CH_{2}$-(O)$OONO_2$	1.1×10^{-11} (298/T) (cm^3 s^{-1})	c
5	$C_xF_{2x+1}CH_2C(O)OONO_2 \rightarrow C_xF_{2x+1}CH_2(O)OO$	2.8×10^{16} exp(T/-13580) (s^{-1})	c
6	$C_xF_{2x+1}CH_2C(O)OO + NO \rightarrow C_xF_{2x+1}CH_2OO$	7.0×10^{-12} exp(T/340) (cm^3 s^{-1})	c
7	$C_xF_{2x+1}CH_2C(O)OO + HO_2 \rightarrow C_xF_{2x+1}CH_2OO$	3.1×10^{-13} exp(T/1040) (cm^3 s^{-1})	c,a
8	$C_xF_{2x+1}CH_2C(O)OO + HO_2 \rightarrow C_xF_{2x+1}CH_2(O)OH$	1.2×10^{-13} exp(T/1040) (cm^3 s^{-1})	c,a
9	$C_xF_{2x+1}CH_2C(O)OO + RO_2 \rightarrow C_xF_{2x+1}CH_2OO$	1.8×10^{-12} exp(T/500) (cm^3 s^{-1})	b
10	$C_xF_{2x+1}CH_2C(O)OO + RO_2 \rightarrow C_xF_{2x+1}CH_2(O)OH$	2.0×10^{-13} exp(T/500) (cm^3 s^{-1})	b
11	$C_xF_{2x+1}CH_2C(O)OH + OH \rightarrow C_xF_{2x+1}CH_2OO$	2.0×10^{-14} exp(T/920) (cm^3 s^{-1})	b
12	$C_xF_{2x+1}CH_2C(O)OO + OH \rightarrow C_xF_{2x+1}C(O)H$	1.1×10^{-14} exp(T/920) (cm^3 s^{-1})	b
13	$C_xF_{2x+1}CH_2OO + HO_2 \rightarrow C_xF_{2x+1}CH_2OOH$	4.1×10^{-13} exp(T/750) (cm^3 s^{-1})	c
14	$C_xF_{2x+1}CH_2OO + NO \rightarrow C_xF_{2x+1}CH_2O$	2.8×10^{-12} exp(T/300) (cm^3 s^{-1})	c
15	$C_xF_{2x+1}CH_2OO + RO_2 \rightarrow C_xF_{2x+1}CH_2O$	1.9×10^{-14} exp(T/390) (cm^3 s^{-1})	b
16	$C_xF_{2x+1}CH_2OO + RO_2 \rightarrow C_xF_{2x+1}CH_2OH$	7.6×10^{-14} exp(T/390) (cm^3 s^{-1})	b
17	$C_xF_{2x+1}CH_2OH + OH \rightarrow C_xF_{2x+1}C(O)H$	1.0×10^{-13} exp(T/-350) (cm^3 s^{-1})	d
18	$C_xF_{2x+1}CH_2OOH + OH \rightarrow C_xF_{2x+1}CH_2OO$	4.0×10^{-12} exp(T/200) (cm^3 s^{-1})	b
19	$C_xF_{2x+1}CH_2O \rightarrow C_xF_{2x+1}OO$	2.5×10^{1} (s^{-1})	d
20	$C_xF_{2x+1}C(O)H + h\nu \rightarrow C_xF_{2x+1}OO$	1.6×10^{-21} (cm^2 $photon^{-1}$ s^{-1})	a
21	$C_xF_{2x+1}C(O)H + OH \rightarrow C_xF_{2x+1}C(O)OO$	6.1×10^{-13} (cm^3 s^{-1})	a
22	$C_xF_{2x+1}C(O)H + Cl \rightarrow C_xF_{2x+1}C(O)OO$	2.8×10^{-12} (cm^3 s^{-1})	a
23	$C_xF_{2x+1}C(O)H + H_2O \rightarrow C_xF_{2x+1}CHOHOH$	1.0×10^{-23} (cm^3 s^{-1})	a
24	$C_xF_{2x+1}CHOHOH + OH \rightarrow C_xF_{2x+1}C(O)OH$	1.2×10^{-13} (cm^3 s^{-1})	a
25	$C_xF_{2x+1}C(O)OO + NO_2 \rightarrow C_xF_{2x+1}C(O)OONO_2$	1.1×10^{-11} (cm^3 s^{-1})	c
26	$C_xF_{2x+1}C(O)OONO_2 \rightarrow C_xF_{2x+1}C(O)OO$	2.8×10^{16} (298/T) (s^{-1})	c
27	$C_xF_{2x+1}C(O)OO + NO \rightarrow C_xF_{2x+1}OO$	8.1×10^{-12} exp(T/-13580) (cm^3 s^{-1})	c
28	$C_xF_{2x+1}C(O)OO + HO_2 \rightarrow C_xF_{2x+1}C(O)OH$	3.1×10^{-13} exp(T/1040) (cm^3 s^{-1})	c,a
29	$C_xF_{2x+1}C(O)OO + HO_2 \rightarrow C_xF_{2x+1}OO$	1.2×10^{-13} exp(T/1040) (cm^3 s^{-1})	c,a
30	$C_xF_{2x+1}C(O)OO + RO_2 \rightarrow C_xF_{2x+1}OO$	1.8×10^{-12} exp(T/500) (cm^3 s^{-1})	b
31	$C_xF_{2x+1}C(O)OO + RO_2 \rightarrow C_xF_{2x+1}C(O)OH$	2.0×10^{-13} exp(T/500) (cm^3 s^{-1})	b
32	$C_xF_{2x+1}OO + NO \rightarrow C_{x-1}F_{2(x-1)+1}OO$	2.8×10^{-12} exp(T/300) (cm^3 s^{-1})	c
33	$C_xF_{2x+1}OO + HO_2 \rightarrow C_{x-1}F_{2(x-1)+1}OO$	4.1×10^{-13} exp(T/500) (cm^3 s^{-1})	d
34	$C_xF_{2x+1}OO + RO_2 \rightarrow C_{x-1}F_{2(x-1)+1}OO$	2.7×10^{-12} exp(T/-470) (cm^3 s^{-1})	c
35	$C_xF_{2x+1}OO + RO_2 \rightarrow C_xF_{2x+1}(O)F$	1.0×10^{-13} exp(T/660) (cm^3 s^{-1})	c
36	$C_xF_{2x+1}C(O)F + H_2O \rightarrow C_xF_{2x+1}C(O)OH$	3.86×10^{-6} (cm^3 s^{-1})	a

a Young and Mabury (2010)

b JPL Data Evaluation (2015) using hydrocarbon analog

c Wallington et al. (2006)

d Yarwood et al. (2007)

Precursor Emissions

$$E^i = f_{use} f_{res} f^i_{hom} f^i_P P_{tot}$$

where for each homolog i, E^i is the total emissions, f^i_{hom} is the fraction of total production accounted for by that homolog, f^i_P is the polymer fraction for the homolog, f_{res} is the fraction of residual precursors in the product, f_{use} is the fraction emitted during use, and P_{tot} is the total fluorotelomer production. f_{res} is assumed to be 0.04 (high scenario) or 0.0028 (low scenario) and f_{use} is assumed to be 1.0 (Wang et al., 2014).

Figure S4. Annual emissions of precursor species by chain length. (left) High emissions scenario (right) Low emissions scenario.

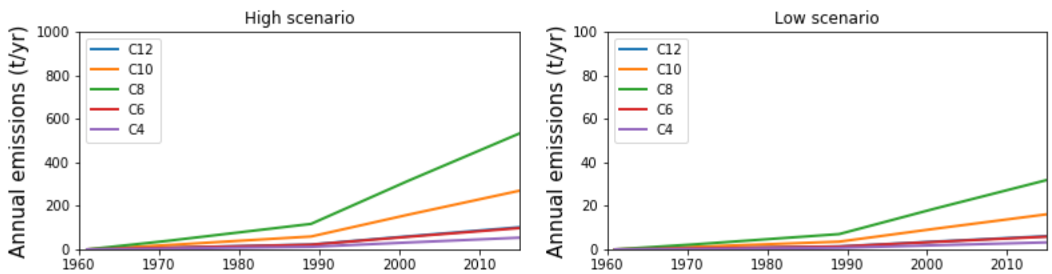

Atmospheric Yields

To calculate atmospheric yields, we used the following procedure. We ran the model with emissions of each homolog for one full year. We then turned off emissions after the first year and continue running model to allow further reaction and deposition. After three years, we sum cumulative depositions of each PFCA (mol) and divide by total emissions (mol) to get yields. This procedure was carried out for each precursor homolog for the simulations NO_HYDR (low) and FTO_ONLY (high) to bound the range of yields

GEOS-Chem info

GEOS-Chem (Bey et al., 2001; http://www.geos-chem.org) uses archived GEOS meteorological data on a rectilinear latitude-longitude grid to compute horizontal and vertical transport. In particular, we use the operational data stream starting in 2012 from the GEOS Forward Processing (GEOS-FP) (native resolution 0.25° x 0.3125°, 72 levels). We run the model at coarse 4°x5° horizontal resolution and 46 vertical levels. GEOS-Chem uses the TPCORE advection algorithm (Lin and Rood, 1996) with the archived meteorological data, and convective transport is computed from the meteorological convective mass flux (Wu et al., 2007). Wet deposition is calculated as described by Amos et al. (2012) and dry deposition by Wesely (1989) and Wang (1998).

Emissions of lightning NO_x (Murray et al., 2012), biogenic VOC (Guenther et al., 2012), and soil NO_x (Hudman et al., 2012) are computed offline based on meteorological conditions.
Anthropogenic emissions default to the global CEDS inventory, except in the US (NEI11v1: Travis et al., 2016), Canada (CAC: van Donkelaar et al., 2008), East Asia (MIX: Li et al., 2014) and Africa (DICE-Africa: Marais and Wiedinmyer, 2016).
The chemistry is simulated using the chemical solver KPP (Damian et al., 2002) through GEOS-Chem's FlexChem interface. Tropospheric HO_x/NO_x/VOC chemistry is coupled to ozone/halogen/aerosol chemistry and follows JPL and IUPAC recommendations.
The GEOS-Chem standard full-chemistry simulation is frequently benchmarked, and these benchmarks can be found online:
http://ftp.as.harvard.edu/gcgrid/geos-chem/1mo_benchmarks/GC_12/
Benchmarking procedures are documented online as well:
http://wiki.seas.harvard.edu/geos-chem/index.php/GEOS-Chem_benchmarking

Code Availability

Model code will be made publicly available at:
https://github.com/cpthackray/global_pfca_simulation_espi

References

Amos, H. M., D. J. Jacob, C. D. Holmes, J. A. Fisher, Q. Wang, R. M. Yantosca, E. S. Corbitt, E. Galarneau, A. P. Rutter, M. S. Gustin, A. Steffen, J. J. Schauer, J. A. Graydon, V. L. St. Louis, R. W. Talbot, E. S. Edgerton, Y. Zhang, and E. M. Sunderland, *Gas-Particle Partitioning of Atmopsheric Hg(II) and Its Effect on Global Mercury Deposition*, Atmos. Chem. Phys., **12**, 591-603, 2012

Bey, I., D. J. Jacob, R. M. Yantosca, J. A. Logan, B. Field, A. M. Fiore, Q. Li, H. Liu, L. J. Mickley, and M. Schultz, *Global modeling of tropospheric chemistry with assimilated meteorology: Model description and evaluation*, J. Geophys. Res., **106**, 23,073-23,096, 2001.

Damian, V., A. Sandu, M. Damian, F. Potra, and G.R. Carmichael, *The Kinetic PreProcessor KPP-A software environment for solving chemical kinetics*, Computers and Chem. Engr., **26**(11), 1567-1579, 2002

Guenther, A.B., Jiang, X., Heald, C.L., Sakulyanontvittaya, T., Duhl, T., Emmons, L.K., and Wang, X., *The Model of Emissions of Gases and Aerosols from Nature version 2.1 (MEGAN2.1): an extended and updated framework for modeling biogenic emissions*, Geosci. Model Dev., **5**, 1471-1492, doi:10.5194/gmd-5-1471-2012, 2012

Hudman, R.C., N.E. Moore, R.V. Martin, A.R. Russell, A.K. Mebust, L.C. Valin, and R.C. Cohen, *A mechanistic model of global soil nitric oxide emissions: implementation and space based-constraints*, Atm. Chem. Phys., **12**, 7779-7795, doi:10.5194/acp-12-7779-2012, 2012

Li, M., Zhang, Q., Streets, D.G., He, K.B., Cheng, Y.F., Emmons, L.K., Huo, H., Kang, S.C., Lu, Z., Shao, M., Su, H., Yu, X., and Zhang, Y., *Mapping Asian anthropogenic emissions of non-methane volatile organic compounds to multiple chemical mechanisms*, Atmos. Chem. Phys., **14**, 5617-5638, doi:10.5194/acp-14-5617-2014, 2014

Lin, S.-J., and R.B. Rood, *Multidimensional flux form semi-Lagrangian transport schemes*, Mon. Wea. Rev., **124**, 2046-2070. 1996

Marais, E. and C. Wiedinmyer, *Air quality impact of Diffuse and Inefficient Combustion Emissions in Africa (DICE-Africa*), Environ. Sci. Technol., 50(19), 10739â€"10745, doi:10.1021/acs.est.6b02602, 2016

Murray, L.T., D.J. Jacob, J.A. Logan, R.C. Hudman, and W.J. Koshak, *Optimized regional and interannual variability of lightning in a global chemical transport model constrained by LIS/OTD satellite data*, , J. Geophus. Res., **117**, D20307, 2012

Travis, K. R., D. J. Jacob, J. A. Fisher, P. S. Kim, E. A. Marais, L. Zhu, K. Yu, C. C. Miller, R. M. Yantosca, M. P. Sulprizio, A. M. Thompson, P. O. Wennberg, J. D. Crounse, J. M. St. Clair, R. C. Cohen, J. L. Laughner, J. E. Dibb, S. R. Hall, K. Ullmann, G. M. Wolfe, J. A. Neuman, and X. Zhou, *Why do models overestimate surface ozone in the Southeast United States*, Atmos. Chem. Phys., 16, 13561-13577, doi:10.5194/acp-16-13561-2016, 2016

van Donkelaar, A., R.V. Martin, W.R. Leaitch, A.M. Macdonald, T.W. Walker, D.G. Streets, Q. Zhang, E.J. Dunlea, J.L. Jimenez, J.E. Dibb, L.G. Huey, R. Weber, and M.O. Andreae, *Analysis of Aircraft and Satellite Measurements from the Intercontinental Chemical Transport Experiment (INTEX-B) to Quantify Long-Range Transport of East Asian Sulfur to Canada*, Atmos. Chem. Phys., **8**, 2999-3014, 2008

Wang, Y., D.J. Jacob, and J.A. Logan, *Global simulation of tropospheric O3-NOx-hydrocarbon chemistry, 1. Model formulation*, J. Geophys. Res., **103**/D9, 10,713-10,726, 1998

Wesely, M.L., *Parametrizations of surface resistances to gaseous dry deposition in regional-scale numerical models*, Atmos. Environ., **23**, 1293-1304, 1989

Wu, X., L. Deng, X. Song, G.J. Zhang, *Coupling of the Convective Momentum Transport of Convective Heating in Global Climate Simulations*, J. Atmos. Sci., **64**, 1334-1349, 2007